Journal of Materials Chemistry B

Accepted Manuscript

ROYAL SOCIETY OF CHEMISTRY

www.rsc.org/materialsB

Journal of Materials Chemistry B

Dynamic Article Links ►

Cite this: DOI: 10.1039/c0xx00000x

ARTICLE TYPE

www.rsc.org/xxxxxx

A new printable and durable *N,O*-carboxymethyl chitosan-Ca^{2+}-polyphosphate complex with morphogenetic activity

Werner E.G. Müller,*[a] Heinz C. Schröder,[a] Meik Neufurth,[a] Emad Tolba,[a,b] Shunfeng Wang,[a] Thorben Link,[a] Bilal Al-Nawas[c] and Xiaohong Wang*[a]

Received (in XXX, XXX) Xth XXXXXXXXX 20XX, Accepted Xth XXXXXXXXX 20XX
DOI: 10.1039/b000000x

Biomimetic materials gain increasing importance in tissue engineering since they may provide regenerative alternatives to the use of autologous tissues for transplantation. In the present study we applied for bioprinting of a functionalized three-dimensional template, *N,O*-carboxymethyl chitosan (*N,O*-CMC), mimicking the physiological extracellular matrix. This polymer, widely used in tissue engineering, has been provided with functional activity by integration of polyphosphate (polyP), an osteogenically acting natural polymer. The two polymers, *N,O*-CMC and polyP, are linked together *via* Ca^{2+} bridges. This *N,O-CMC+polyP* material proved to be printable and durable. The *N,O-CMC+polyP* printed layers and tissue units retain their property to induce SaOS-2 bone-like cells to biomineralization. Subsequent *in vivo* experiments revealed a strong regeneration-inducing activity of the material in the rat calvarial defect model. In turn, *N,O-CMC+polyP* represents a promising hybrid material useful as potential custom-designed scaffold for alternative tissue-engineering solutions.

1. Introduction

Biological bone substitutes must meet the requirements to be highly porous and to offer a suitable microenvironment for regenerative cells, supporting cell attachment, proliferation and differentiation, as well as of initiating/maintaining neo-tissue genesis. In bone tissue engineering, various metals have been applied for fabrication of three-dimensional (3D) scaffolds. In spite of their favorable mechanical properties, metals have the disadvantage not to be biodegradable[1,2]. In parallel, inorganic/ceramic materials, e.g. hydroxyapatite (HA) or calcium phosphates, have been developed that show the desired osteo-conductivity, but are brittle[3] and difficult to produce in a highly porous structure. Finally, biomimetic artificially designed scaffolds for tissue engineering have been developed that mimic crucial features of the natural extracellular matrix to induce proliferation and differentiation of adult/embryonic stem cells and to allow cell recruiting/seeding during neo tissue genesis. Among the naturally occurring polymers, chitosan derived by deacetylation from chitin, the second most abundant biopolymer, shows outstanding biomedical properties, being both biocompatible and biodegradable, and by that predestined to act as a suitable matrix for the fabrication of either 3D-scaffolds, as gels and tissue-like units, and as 2D-scaffolds, as films and fibers[4]. Chitosan has been frequently used as space-filling implants. However, this natural polymer has to be processed with morphogenetically active components, e.g. silica, to become a suitable morphogenetically active matrix for bone regeneration[5].

Previously we disclosed the role of polyphosphate (polyP), a natural polymer synthesized in platelets[6], during HA deposition[7-9], as a morphogenetically active polymer acting on bone cells and their precursors. Therefore, it was tempting to complex polyP with chitosan in order to develop a biomimetic material that can be composed and even bioprinted to tissue-like units with a controlled morphology that display the favored biological activity. Since chitosan, a polysaccharide randomly built by β-(1-4)-linked D-glucosamine and *N*-acetyl-D-glucosamine units, cannot form a complex with polyP at physiological conditions we had to derivatize chitosan to *N,O*-carboxymethyl chitosan (*N,O*-CMC)[10,11]. The ampholytic character of *N,O*-CMC provides this polymer with an ample of applications[12]. In the present study we compose a formula for the preparation of a bioprintable material, composed of alginate[13], *N,O*-CMC and, the Na^+ salt of polyP (Na-polyP). In this scaffold *N,O*-CMC and also alginate act as structure-guiding polymers that undergo controlled hardening in the presence of divalent cations (**Fig. 1**). After having printed this material to custom-designed/fabricated layers and implants the structures were exposed to Ca^{2+} in order to harden them and to make those scaffolds more durable. During Ca^{2+} exposure the Na^+ cations in polyP are exchanged by Ca^{2+} allowing the bridging of polyP to *N,O*-CMC and rendering this composite material to a persistent structure and morphology, without losing the biological activity of polyP. The organization of this polyP-*N,O*-CMC composite material to durable tissue-like moldable blocks has been achieved by alginate, a natural polymer, composed of unbranched chains of (1,4) linked β-D-mannuronate and α-L-guluronate residues arranged in a blockwise fashion[14]. This polymer can form, *via* electrostatic forces between the carboxyl groups within the alginate and the counterion species (e.g. Ca^{2+}), gels of a controlled strength and porosity[15]. Based on these

properties we describe a formula for a matrix (*N,O*-CMC, polyP and alginate) that can be bioprinted as soft, moldable 3D structures. Those 3D printed molds are, in the subsequent fabrication stage, hardened by exposure to Ca^{2+} (**Fig. 1**). In the present study, this scaffold had been examined also *in vivo* to determine the regeneration potential of this matrix. Those studies had been performed with beads/implants, containing either β-tri-calcium phosphate (β-TCP), or β-TCP together with silica, or *N,O*-CMC together with polyP. The β-TCP implants have been chosen as a control (reference material) in view of the established beneficial activity of this calcium salt of phosphoric acid during bone formation[16]. In view of earlier studies revealing that Ca^{2+}-alginate did not display *in vitro* mineralization-inducing effect on SaOS-2 cells[17], while β-TCP induced in those cells a strong increase of ALP activity[18,19], we did not include *N,O*-CMC or alginate/$CaCl_2$ hydrogel (without polyP) as a reference control into the animal studies, presented here.

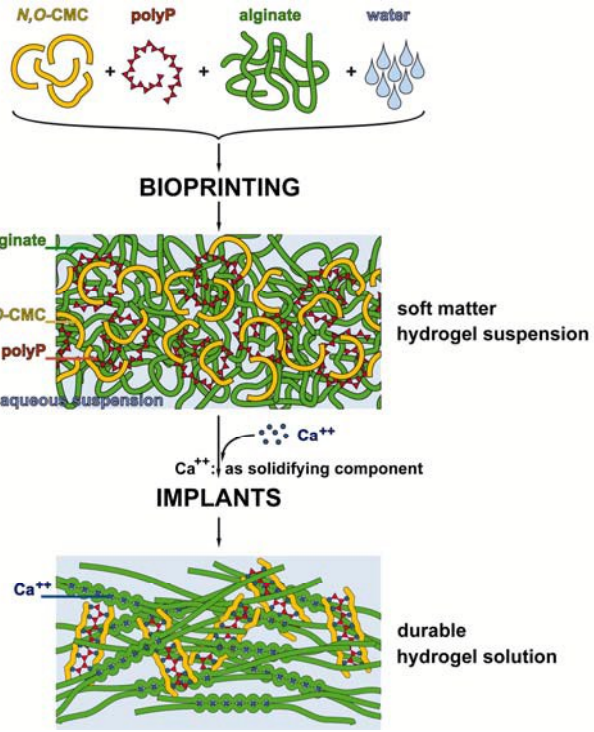

Fig. 1 Organizing potential of Ca^{++} added to a suspension formed of dissolved *N,O*-CMC, solid Na-polyP and aqueous alginate. It is sketched that in the absence of Ca^{2+} the polymers *N,O*-CMC, Na-polyP and alginate are present as random-coiled structures. This material can be bioprinted. After addition of Ca^{2+}, the cation binds to the stretches of sugar anions (α-L-guluronate residues) under formation of alginate fibers that organize and orient the *N,O*-CMC as well as the Ca^{2+} salt of polyP to durable implants.

In addition, silica implants together with β-TCP have been tested, since recent studies showed the increase of the regeneration potential of β-TCP by silica *in vivo*, in rabbits[20]. In a third series of experiments, polyP, as a morphogenetically active polymer, was included into the beads together with *N,O*-CMC. *N,O*-CMC was used as the charged structural polymer in order to stabilize polyP via Ca^{2+} ionic bridges. The suitability of chitosan and *N,O*-CMC derivatives have been proven to serve as suitable carriers for bioactive, anabolic bone components[21].

In order to allow a direct correlation of the bioactivity (bone regeneration-promoting activity) of the new scaffold material, developed here, the biomaterial had been fabricated into microspheres. Using those beads we could recently establish that both silica and β-TCP cause an accelerating effect on bone regeneration in rabbits[20].

2. Materials and Methods

2.1 Preparation of *N,O*-carboxymethyl chitosan

N,O-carboxymethyl chitosan (*N,O*-CMC) was prepared from chitosan as described[10,22,23]. In brief, 10 g chitosan (C3646 Sigma; from shrimp shells, ≥75% (deacetylated) [deacetylated chitin]) was added to a water:isopropanol mixture (20 ml : 40 ml) containing 14.1 g NaOH and kept at room temperature for 1 h under mild stirring. After that, 15 g of monochloroacetic acid dissolved in 20 ml of isopropanol was added to the mixture dropwise. The reaction mixture was heated to 50°C and stirring was continued for 4 h. Then the material was filtered and washed three times with 80% ethyl alcohol. The resulting solid was dried overnight in an oven at 60°C to obtain the Na salt of *N,O*-CMC. For the conversion to the H-form of *N,O*-CMC, the obtained powder was suspended in 100 ml of aqueous 80% ethyl alcohol solution. Then 10 ml hydrochloric acid (37%) was added and stirred for 30 min. Finally, the suspension was filtrated and washed with ethyl alcohol until a neutral pH was obtained; the material was dried at 60°C overnight[23]. A schematic outline of the reaction is given in Fig. 1.

Fourier transformed infrared (FTIR) spectroscopy has been used in the attenuated total reflectance (ATR) mode to assure the substitutions of carboxymethyl groups at the amino group as well as the primary hydroxyl sites of chitosan (FTIR-ATR; Varian 660-IR spectrometer with Golden Gate ATR auxiliary)[10]. Dried powder of sample was placed onto the ATR crystal directly.

2.2 Printing of N,O-CMC-polyphosphate layers and tissue-like-blocks

Na-polyphosphate (Na-polyP of an average chain of 40 phosphate units) was obtained from Chemische Fabrik Budenheim (Budenheim; Germany).

N,O-CMC was sterilized by ultraviolet radiation (254 nm) overnight. Then a solution of 60 mg/ml *N,O*-CMC was prepared in physiological saline (P3813; Sigma; Steinheim; Germany). After stirring until being homogenous the gel was supplemented with solid Na-polyP until the concentration of 20 mg/ml was reached. The hydrogel preparation formed was completed with 60 mg/ml of Na-alginate (W201502; Sigma-Aldrich) and stirred at 50°C until it became homogenous. The hydrogel obtained was filled into sterile 30 ml printing cartridges (Nordson EFD, Pforzheim; Germany) and centrifuged for 3 min at 1500 rpm to remove remaining air bubbles. After connecting the 0.25 mm tapered polyethylene printing tip (Nordson EFD, Pforzheim; Germany) the cartridge was placed into the preheated (25°C) printing head of the 3D-Bioplotter™ (4th generation blotter; Envisiontec, Gladbeck; Germany).

Bioprinting was performed, essentially as described[13]. The printing solution, composed of 60 mg/ml of *N,O*-CMC, 60 mg/ml of alginate and 20 mg/ml of Na-polyP was prepared at 25°C using a pressure of 1.4 bar and a printing speed of 18 mm/s. The pre-flow was set to 0.15 s whereas the post-flow amounts to -0.05 s. Cylindrical scaffolds measuring 50 × 0.4 mm were designed, sliced and transferred to the printer software as described[13]. The strand distance between the printed cylinders was set to 1 mm, resulting in a pore size of the printed layers/blocks of approximately 0.5 × 0.5 mm. Those scaffolds, layers/blocks, were printed directly into sterile 94 mm Petri dishes (Greiner Bio-One, Frickenhausen; Germany), supplemented with 1% [w/v] $CaCl_2$ as cross-linking solution, as described[17]. After a ≈2 min incubation period the $CaCl_2$-solution was drained and the cross-linked scaffolds produced were washed twice with distilled water and once with 70% ethanol. The printing of a two layered scaffold with 5 cm in diameter lasted approximately 6 min. The size of the scaffold samples for the cell culture experiments was 20 mm [diameter] × 0.4 mm [thickness].

A tissue-like block was printed after analysis of the cranial defect a pig underjaw had been selected, by microtomography [μCT][24]. The implant dimensions to be printed were predetermined using the computer program Bioplotter RP 2.9 CAD software (Envisiontec, Gladbeck; Germany). Using the same software, the cylinders were subsequently sliced to individual layers corresponding to the diameter of the printing needle and subsequently transferred to the VisualMachines 3.0.193 printer software (Envisiontec, Gladbeck; Germany).

2.3 Preparation of *N,O*-CMC hydrogel layer

For this comparative study *N,O*-CMC hydrogel was prepared as described[22,25,26]. The solid material prepared was layered on the Petri dish (termed "*N,O*-CMC hydrogel").

2.4 Scanning electron microscopy and energy-dispersive X-ray spectroscopy

The scanning electron microscope (SEM; HITACHI SU 8000) was coupled to an XFlash 5010 detector, an X-ray detector that allows simultaneous energy-dispersive X-ray (EDX)-based elemental analyses[13]. This was coupled at voltage of 4 kV to the XFlash 5010 detector that was used for element analysis. HyperMap databases were collected, as described by Salge and Terborg[27].

2.5 Determination of the hardness of the *N,O-CMC+polyP* scaffold

The hardness of the scaffolds was quantified by a ferruled optical fiber-based nanoindenter as described[28,29]. The indents were depth controlled (10 μm) and the loading and unloading period was set to 2 s. Based on the load-displacement curves, obtained by the nanoindenter equipped with a ferruled optical fiber system (Optics11, Amsterdam; The Netherlands), the reduced Young's modulus [RedYM] was calculated[30].

2.6 Light microscopic analyses

Digital light microscopic studies were performed using a VHX-600 Digital Microscope (Keyence, Neu-Isenburg; Germany) equipped with a VH-Z25 zoom lens.

2.7 Mineralization by SaOS-2 cells *in vitro* on chitosan matrices

Human osteogenic sarcoma cells, SaOS-2 cells[31] were used for the experiments. They were cultivated in McCoy's medium in a humidified incubator at 37°C and 5% CO_2, as described[32]. Culture medium/fetal calf serum [FCS] was changed every 3 d. Where mentioned the cells (3×10^4 per well) were exposed to the osteogenic cocktail [OC], containing 10 nM dexamethasone, 5 mM β-glycerophosphate and 50 mM ascorbic acid[32]. The scaffold samples 20 mm [diameter] × 0.4 mm [thickness] were placed to the bottom of the 24-well pates.

The extent of mineralization was assayed by Alizarin Red S and measured spectrophotometrically[33]. Prior to the measurement the chitosan matrices were removed from the 40-well plates. The amount of bound Alizarin Red S is expressed in nmoles and correlated to total DNA in the samples.

2.8 Induction of *alkaline phosphatase* gene in SaOS-2 cells *in vitro* on *N,O*-CMC matrices, supplemented with polyP.

The scaffold, composed of 60 mg/ml of *N,O*-CMC, 60 mg/ml of alginate, in the absence or presence of 20 mg/ml of Na-polyP, was printed in layers/blocks as described above. For hardening of the material the layers/blocks were exposed (≈2 min) either to 1% [w/v], or to 2.5% [w/v] $CaCl_2$ solution as cross-linking solution, as described here. The scaffolds obtained were washed twice with distilled water and once with 70% ethanol, placed into the 24-well plates. Then the samples were overlayed with 3 ml of a SaOS-2 cell suspension (3×10^4 per well). After an initial incubation period of 3 d the assays were incubated in medium/FCS with the OC and additionally incubated for 1 d, 5 d or 8 d. Then RNA was extracted and subjected to quantitative real-time RT [reverse transcription]-PCR (qRT-PCR) as described[34]. The expression of the *alkaline phosphatase* (ALP) gene had been measured by using the primer pairs described[33]. The expression level of the *ALP* had been normalized to the one of the reference gene GAPDH (glyceraldehyde 3-phosphate dehydrogenase)[34].

2.9 Ethics statement

The animal procedures had been approved by the Dongzhimen Hospital at the Beijing University of Chinese Medicine, No. 5 Haiyuncang Road, Dongcheng District, Beijing 100700, China, and performed by Dr. Xing YU. The certificate number is 2012-0001, granted from the Beijing Committee of Science and Technology.

2.10 Preparation of microspheres

The preparation of the PLGA [poly(D,L-lactide-*co*-glycolide)]-based microspheres was as described before[20,35]. Two kind of spheres were prepared; The 820 ± 27 μm large "*β-TCP-micro*" beads, containing 7.92 ± 0.20% of β-TCP, and the "*β-TCP/Silica-micro*" beads measuring 825 ± 30 μm, and containing 4.97 ± 0.24% β-TCP and 9.38 ± 0.53% for silica. β-Tri-calcium phosphate (β-TCP) has been obtained from Sigma (49963; Taufkirchen; Germany). The resp. beads were pressed to 1.5 mm thick discs of a diameter of 10 mm.

The preparation of the hydrogel discs, composed of 60 mg/ml of *N,O*-CMC and 60 mg/ml of Na-alginate, was performed as described above. The hydrogel was applied in the absence (*N,O-CMC-polyP*) or presence of 20 mg/ml of Na-polyP ("*N,O-CMC+polyP*"). The gel was passed through a 0.2 mm needle hooked to a syringe and dropped into a 2.5% [w/v] $CaCl_2$ solution, supplemented with 70% ethanol. After washing with physiological saline the spheres could be collected. Subsequently, the pearls were likewise pressed to discs (1.5 mm × 9 mm).

2.11 Surgical procedures – Animal study

The male Sprague-Dawley rats, 6 weeks old (180 ± 25 g), were obtained from the Animal Resources Centre (Dongzhimen Hospital, Beijing University of Chinese Medicine, Beijing 100700, China). After acclimatization for two weeks to local vivarium conditions before surgery the animals were anesthetized by intraperitoneal injection with 10% chloral hydrate (3.0 ml/kg; C8383; Sigma). The surgical procedure followed, applying a described procedure[36]. After shaving and disinfecting of the surgical site, the dorsal surface of the cranium, a 3-cm midline incision was set over the calvaria, the skin was left open with retractors, the periosteum was fixed aside, and the periosteum was removed from the surface of the cranial bone by scraping. Then a 10-mm craniotomy critical size defect was drilled into the calvarium with a surgical drill and trephine operating at 1200 rpm. This size was chosen to ensure that the defect does not completely heal over the natural lifetime of an animal, as proposed[36]. Extreme care was taken to avoid any damage of the dura mater.

Into the opened calvaria the respective discs (weight 0.23 ± 0.04 g) were inserted into the bone defect. Then, the skin was closed using 4-0 silk sutures and the rats were given an intramuscular injection of an analgesic (0.05 mg/kg buprenorphine) and allowed for unrestricted cage activity. After 56 d the animals were euthanized with inhaled CO_2 and the calvaria was removed for histological analysis. The animals had been randomly divided into three groups (4 specimens in each group) and one rat received one disc each as follows: in group 1, "*β-TCP-micro*"-, group 2 "*β-TCP/Silica-micro*"-, and group 3 "*N,O-CMC+polyP*" disc with microspheres.

2.12 Histological analysis

The respective calvariae were fixed overnight with 10% formaldehyde and the specimens were decalcified in 0.5% formaldehyde containing 10% EDTA (pH 7.4), dehydrated in a graded increasing alcohol series and finally embedded in paraffin; 5 µm thick sections (collaterally and bridging the bone-defect region) were prepared and stained with Masson's trichrome[37]. The mineralized collagen and bone areas are in green or blue, while the muscle fibers and keratin light up in red; the cell nuclei appear in black. Randomly selected fields were observed with an Olympus IX71 microscope.

2.13 Mechanical properties of the regenerating bone tissue

Samples from the collaterally and bridging the bone-defect region were removed and fixated with Karnovsky solution[38]. The bone samples were sliced with a diamond saw, followed by lightlywet-polishing, as described[20]. The mechanical properties of the regenerating zone, bone-defect region, between the pre-existing bone and the new bone tissue were determined on the basis of load-displacement curves using reduced Young's modulus [RedYM][30].

2.14 Statistical analysis

The results were statistically evaluated using paired Student's *t*-test[39]. In the region between the pre-existing bone and the newly regenerated bone tissue, 40 individual measurements, from 4 separate animals, were performed. The lower and upper limits (whiskers) were set to 2.5th and 97.5th percentile, according to the Statistical Package for the Social Sciences version 11.0[40,41].

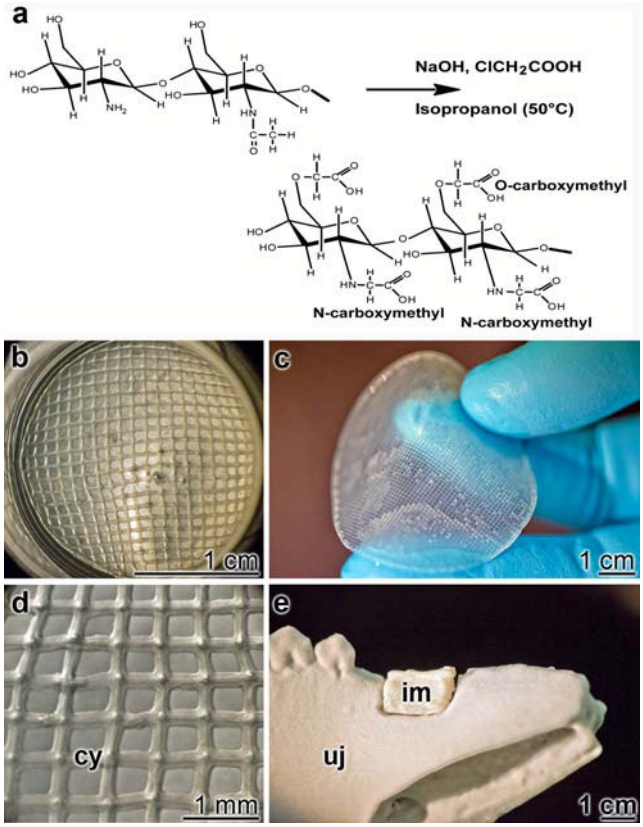

Fig. 2 Formation of *N,O-CMC+polyP* membranes and tissue units. (**a**) Chitosan, characterized by the D-glucosamine (deacetylated) and *N*-acetyl-D-glucosamine (acetylated) units, is converted into *N,O*-CMC by carboxymethylation of the polymer. (**b** to **e**) Mats of two (b and c) to six layers (d) were bioprinted; the orthogonal arrangement of the printed cylinders (cy) is distinct. (e) Printing of a *N,O-CMC+polyP* tissue-like unit, an implant (im), formed according to the lesion in a pig underjaw (uj).

3. Results and Discussion

3.1 Synthesis and characterization of the *N,O-CMC+polyP* scaffold

N,O-CMC was prepared from chitosan by reaction with monochloroacetic acid in an alkaline environment (sodium hydroxide) and in the presence of isopropanol (**Fig. 2a**). Solid Na-polyP was mixed with a *N,O*-CMC solution, until the concentration of 20 mg/ml was reached; then 60 mg/ml Na-

alginate was added. Starting from *N,O*-CMC a new *N,O-CMC+polyP* scaffold, in the Na-alginate hydrogel, was fabricated, by blending of *N,O*-CMC with Na-polyP. Using the setting applied here, two or six layers were printed and used for the *in vitro* studies. In **Fig. 2b** and **Fig. 2c** the two-layer mats are shown that have been incubated with bone-like SaOS-2 cells or with human blood. The mesh size of the cylinders within one layer was ≈0.5 × 0.5 mm (**Fig. 2d**). The thickness of the layers can be enlarged by increasing the numbers of layers. A six-layer pad is shown in **Fig. 2c**. Increasing further the number of layers in the plies, tissue-like blocks are formed (Fig. **2e**). By using this layer-by-layer printing approach a cranial defect in a pig underjaw, after having analyzed the lesion by µCT, has been fabricated from the *N,O-CMC+polyP* scaffold and hardened by Ca^{2+}.

The surfaces of the membranes, layers or tissue-like-blocks, formed by *N,O*-CMC and Na-polyP in Na-alginate and linked together *via* Ca^{2+} ionic bridges, were inspected microscopically and found to be most widely even; the surface roughness does not exceed 1 µm (**Fig. 3a** and **Fig. 3b**). The samples were analyzed for the presence of phosphorus by EDX spectroscopy. As an example the EDX spectra from membranes, prepared without Na-polyP and with Na-polyP are given (**Fig. 3c** and **Fig. 3d**). The spectra revealed that the membranes formed in the presence of Na-polyP and linked *via* Ca^{2+} to the *N,O*-CMC polymer show the signals for phosphorous (P) and calcium (Ca) (**Fig. 3d**), while the signal for P is absent in the membranes formed in the absence of polyP (**Fig. 3c**).

FTIR spectral analysis had been performed with both chitosan (**Fig. 4a**) and *N,O*-CMC (**Fig. 4b**). The spectra were acquired at 4000-750 cm^{-1} wave numbers with a 4 cm^{-1} resolution. The chitosan FTIR spectrum (**Fig. 4a**) shows a broad peak in the region 3600 and 3000 cm^{-1} which is attributed to the O–H stretching vibration, N–H extension vibration as well as the intermolecular H-bonds of the polysaccharide moieties. The two bands at 2915 and 2840 cm^{-1} correspond to the C–H stretching. The bands at 1586 cm^{-1} (N-H bend) and 1659 cm^{-1} (C=O stretch) are intrinsic peaks for chitosan and the bands at 1410 and 1380 cm^{-1} were assigned to the C–H symmetrical deformation mode. Moreover, the band at 1158 cm^{-1} represents the bridging oxygen of C–O–C stretch and the bands between 1000 and 1100 cm^{-1}, indicating non bridging oxygen C–O–H stretch due to primary (CH_2–OH in primary alcohols) and secondary hydroxyl group (–CH–OH in cyclic alcohols) of chitosan. **Fig. 4b** shows the characteristic peaks of *N,O*-CMC. Compared to the peaks of chitosan, the peaks of *N,O*-CMC at 1590 cm^{-1} and 1380 cm cm^{-1} correspond to the carboxyl group (which overlaps with N–H bend) and the carboxymethyl group, respectively. In addition the intensities of the primary and secondary hydroxyl groups at 1000-1100 cm^{-1} are also changed. Following the literature[10], these features are taken as evidence that the carboxymethylation occurred at the hydroxyl as well as the amino groups of chitosan. Likewise the changes of the intensities of the primary and secondary hydroxyl groups are indicative for the carboxymethylation on the primary hydroxyl group CH_2OH at the C6 position.

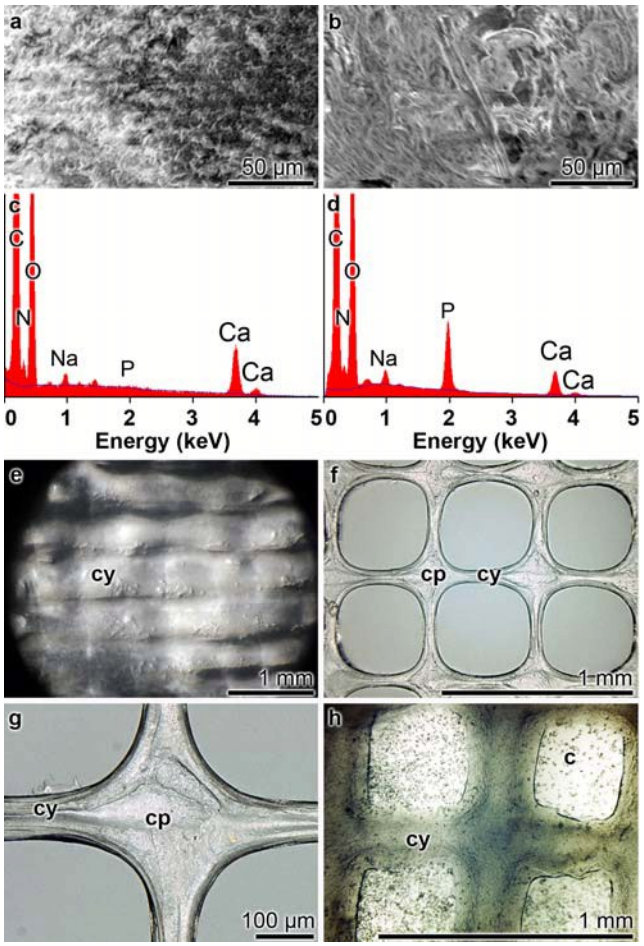

Fig. 3 Effect of Ca^{2+} on the integrity of the printed cylinders, formed of *N,O*-CMC and Na-alginate in the absence or presence of polyP. (**a** to **d**) EDX analysis of membranes formed of *N,O*-CMC. The membranes were prepared in the absence of polyP (a and c) or in the presence of polyP (b and d). (a and b) The surfaces of the membranes are even. (c) The EDX spectrum of the *N,O*-CMC, in the absence of polyP, is lacking the signal for phosphorus (P). (**e** to **h**) Integrity and stability of the *N,O-CMC+polyP* meshwork. The scaffold meshes build from (e) *N,O*-CMC, not containing polyP, are composed of cylinders (cy) that fuse along the complete structures. (f and g) In contrast, the *N,O-CMC+polyP* meshes with their cylinders (cy) remain intact even if submersed in culture medium. In the freshly prepared *N,O-CMC+polyP* meshwork their cylinders fuse at the crossing points (cp). (h) Even after an incubation period of the *N,O-CMC+polyP* mesh in culture medium for 5 d, the cylinders (cy) remain separated and allow the cells (c) to proliferate in the open space and also onto the cylinders.

The degree of *N,O*-carboxy methyl substitution in chitosan was determined by potentiometric titration[22, 42] and found to be ≈ 0.84.

Determination of the mechanical properties of the biopolymer material (alginate-Ca^{2+}-*N,O*-CMC+polyP) revealed a hardness (elastic modulus) of 475 kPa even after a short (5 min) incubation in the $CaCl_2$ solution that can be further increased by a

prolongation of the incubation period or addition of ethanol (to be published). These determinations had been performed with the ferrule-top nanoindenter, described under "Materials and Methods".

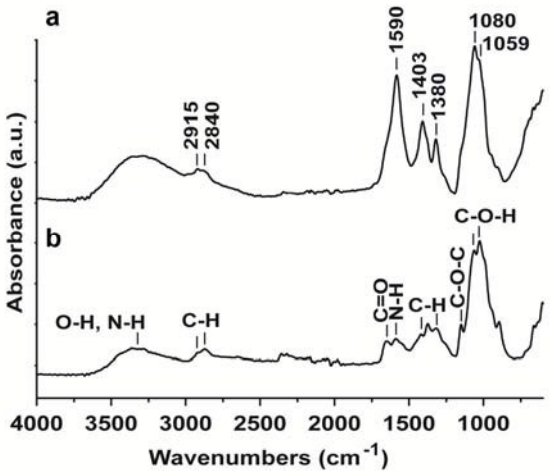

Fig. 4 FTIR spectra of chitosan (**a**) and *N,O*-CMC (**b**).

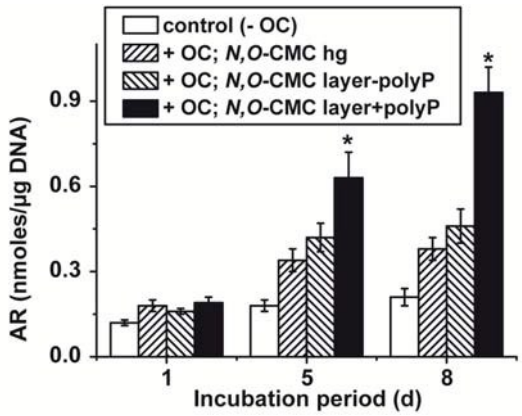

Fig. 5 Biological/morphogenetic activity of *N,O-CMC+polyP*, *N,O*-CMC containing polyP, versus polyP-free scaffold determined in bone-like SaOS-2 cells to mineralize on chitosan matrices. The SaOS-2 cells were grown in the absence (control; -OC [osteogenic cocktail]) or presence of the +OC. In the latter series of assays the cells were cultured on the previously published *N,O*-CMC hydrogel (*N,O*-CMC hg)[19], or on *N,O*-CMC layers, in the absence (*N,O-CMC-polyP*) or presence of polyP (*N,O-CMC+polyP*). The extent of biomineralization (Alizarin Red S [AR]) is correlated with the DNA content in the assays. Values represent the means (± SD) from 10 separate experiments each. It is seen that on the *N,O-CMC+polyP* matrix a significant increase in mineralization occurred; $*P < 0.01$.

3.2 Bioprinting of the *N,O-CMC+polyP* scaffold and biomineralization of SaOS-2 cells

The two layer printed scaffolds were used for cell culture experiments. If a sample from a *N,O*-CMC layer, lacking any polyP, has been printed the cylinders fuse along their entire surfaces in the culture medium (**Fig. 3e**). In contrast, if this material to be printed is supplemented with polyP, *N,O-CMC+polyP*, the cylinders remain separated (**Fig. 3f** and **Fig. 3g**). Interestingly enough at the crossing sites of the cylinders an intimate fusion is observed and pronounced crossing points are formed that build a continuous mesh (**Fig. 3f** and **Fig. 3g**). The distinct intersections between the printed cylinders leave room for the infiltration of cells (**Fig. 3h**). Even after a five days' incubation period the meshwork remain intact (**Fig. 3h**).

The hardness of the *N,O-CMC+polyP* scaffold was measured with an indenter device and using a cantilever on the top of a glass ferrule. Scaffold samples of 6 layers with a thickness of 2 mm were analyzed. The samples that had been obtained immediately after printing were submersed into saline and tested for the hardness, using the reduced Young's modulus [RedYM] as a parameter. If those samples, *N,O-CMC+polyP*, were analyzed a mechanical RedYM stiffness of 935±128 kPa was determined (n=10); in contrast, the samples from the scaffold lacking polyP (*N,O*-CMC) measured only 27 ± 3 kPa. In comparison and using the same settings the trabecular bone from a rabbit tissue was found to have a modulus of 2,300 kPa[17]. Submersing the *N,O-CMC+polyP* scaffold samples in simulated body fluid[43] the RedYM stiffness changed not significantly during a 3 weeks' period; the values were around 900 ± 115 kPa. Only after 6 weeks a significant reduction of the RedYM to 686 ± 102 kPa was measured.

The matrices, prepared here, *N,O*-CMC without and with polyP, as well as (by way of comparison) the chitosan preparation, termed *N,O*-CMC hydrogel, published earlier[22,25], were tested for their potency to induce biomineralization in SaOS-2 cells. The cells were transferred after an initial incubation period for 3 d in medium/FCS supplemented with the osteogenic cocktail, OC. As shown in **Fig. 5**, *N,O-CMC+polyP*, which contains polymeric polyP bound to the *N,O*-CMC, caused a significantly higher induction of the mineralization of the cells (0.93 ± 0.09 nmoles of Alizarin Red S bound to the cells [based on µg of DNA] at day 8) than *N,O*-CMC matrices, lacking polyP. This holds true for the published *N,O*-CMC hydrogel matrix (0.38 ± 0.04 nmoles/µg) and the matrix prepared in the present study (0.46 ± 0.06 nmoles/µg). In the absence of any chitosan matrix the extent of mineralization was 0.38 ± 0.07 nmoles/µg (not shown in **Fig. 5**). In the absence of OC (osteogenic cocktail) the level of mineralization was low with ≈ 0.20 ± 0.03 nmoles/µg (**Fig. 5**).

3.3 Enhanced *in vitro* gene expression of *alkaline phosphatase* after by polyP

SaOS-2 cells were incubated in the presence of OC onto the printed matrices, composed of 60 mg/ml of *N,O*-CMC, 60 mg/ml of alginate, in the absence or presence of 20 mg/ml of Na-polyP. The samples were hardened with 1% [w/v], or with 2.5% [w/v] $CaCl_2$ solution, as described under "Materials and Methods". As summarized in **Fig. 6**, no significant difference in the expression ratio between the *ALP* and the *GAPDH* is measured for the different matrices 1 d after addition of the OC medium. The levels vary around a ratio of 0.027. After a 5 d incubation period the value for the ratio ALP:GAPDH increases in the assays with the *N,O*-CMC matrix in the absence of polyP and hardened in 1% $CaCl_2$ to 0.043±0.006 and after 8 d to 0.069±0.008; no significant

differences is seen if the matrix had been hardened with 2.5% $CaCl_2$ (data not shown). If the *N,O*-CMC matrices had been supplemented with polyP a significant increase of the expression levels is measured after an incubation period for 5 d and even more for 8 d, irrespectively of the concentration of $CaCl_2$ solution which had been used for hardening the matrices (**Fig. 6**).

These data underscore and support earlier findings that polyP, if present also in the *N,O*-CMC matrix, described here, induce the expression of the *ALP* gene. It is well established that this enzymes is amplified during the activation of osteoblasts and during the biomineralization process proceeding in those cells[9].

The viability of the cells onto the matrices, composed of *N,O*-CMC, in the absence or presence of polyP, did not change significantly (data not shown). The viability had been determined with trypan blue[17].

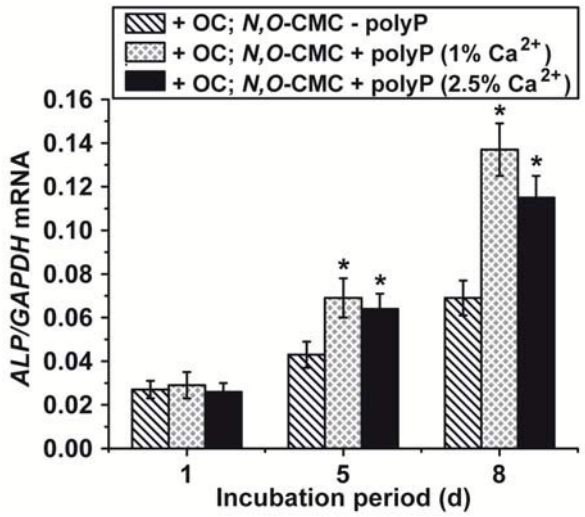

Fig. 6 Effect of polyP in the *N,O*-CMC matrix on the gene expression of the *ALP*. SaOS-2 cells were incubated in the presence of the OC onto *N,O*-CMC layers either in the absence of polyP (*N,O*-CMC-polyP) or presence of this polymer (*N,O*-CMC+polyP). The *N,O*-CMC-polyP sample was hardened with 1% $CaCl_2$; the corresponding *N,O*-CMC+polyP samples had been hardened either with 1% , or with 2.5% $CaCl_2$, as indicated. After an incubation period of 1 d, 5 d or 8 d the cells had been harvested, subjected to RNA extraction and finally to quantitative real-time RT-PCR (qRT-PCR) analysis for both *ALP* mRNA and *GAPDH* transcripts. The expression level of *ALP* was normalized to the expression of *GAPDH*. Data are expressed as mean values ± SD of five independent experiments; each experiment had been carried out in duplicate. Differences between the group, lacking polyP (*N,O*-CMC-polyP) and those samples that had been grown onto the *N,O*-CMC layers, supplemented with polyP (*N,O*-CMC+polyP), were evaluated using an unpaired t-test, $*P < 0.05$.

3.4 *In vivo* biomineralization activity of the *N,O-CMC+polyP* scaffold

The promotion of bone regeneration by the new *N,O-CMC+polyP* scaffold was studied *in vivo*, using the rat calvarial defect model, as described[36]. After setting an 10 mm large defect

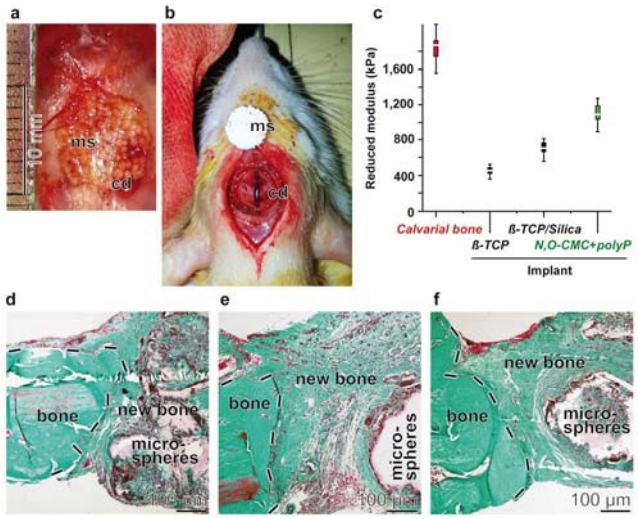

Fig. 7 *In vivo* anabolic activity of the "*N,O-CMC+polyP*" scaffold. The animals studies had been performed as described under "Materials and Methods". (**a** and **b**) At the dorsal surface of the cranium of rats incisions were set and then holes drilled. In such a cranial bone defect (cd) a disc, composed of different microspheres (ms), was implanted. After 56 d the regenerating regions were analyzed. (**c**) Box plot comparing the stiffness/RedYM of the calvarial bone, "*β-TCP-micro*" beads with β-TCP alone, "*β-TCP/Silica-micro*" beads, containing both β-TCP and silica, as well as "*N,O-CMC+polyP*" microspheres, composed of the *N,O*-CMC, solid Na-polyP and aqueous alginate. After the 56 d-implantation period the animals were sacrificed, sections along the pre-existing bone-regenerated new bone area were prepared. Then the mechanical properties of the calvarial, pre-existing bones (from animals which had obtained "*β-TCP-micro*" beads), as well as from the new regenerated bone regions between the microspheres implants and the pre-existing bones were determined. The stiffness/RedYM of the new-formed bone regions around the "*β-TCP-micro*", "*β-TCP/Silica-micro*" beads, as well as the "*N,O-CMC+polyP*" microspheres were determined using the ferrule-top nanoindenter. Whiskers lower and upper limits were set to 2.5th and 97.5th percentile. The horizontal bars within the box indicate the median value. (**d** to **f**) Histological evaluation. The animals were implanted in the cranium with the discs, composed of microspheres containing either "*β-TCP*" alone, "*β-TCP-micro*" beads, or both β-TCP and silica, the "*β-TCP/Silica-micro*" beads, and finally the microspheres, prepared from the newly developed material, the "*N,O-CMC+polyP*" scaffold. After an implant period for 56 d, the animals were sacrificed and sections through the zone of pre-existing bone-new bone within the implant region, the dorsal surface of the cranium, set over the calvaria, were prepared. The sections were stained with Masson's trichrome; by that the mineralized regions are stained in green, while the non-mineralized tissue (muscle fibers and keratin) are stained in red. The regions of the pre-existing bone, of the newly, regenerated bone and the implanted microspheres are marked. Representative sections through implants with (g) "*β-TCP*", (h) "*β-TCP/Silica*", or (i) "*N,O-CMC+polyP*" scaffold are shown here.

in the dorsal surface of the cranium over the calvarium the implant sample (**Fig. 7a)**, microspheres, was placed into the hole, following a procedure, described by us recently[20] (**Fig. 7b**). The size of the implanted spheres was 10 mm × 1.5 mm. The ≈ 0.23±0.04 g weighing implants were composed of microspheres that had been prepared by controlled, dropwise addition of the

N,O-CMC+polyP scaffold into 70% ethanol, containing 2.5% [w/v] $CaCl_2$; **Fig. 8b**. Following this procedure the hardness (mechanical RedYM stiffness) of the spheres increased to 1.22 ± 0.31 MPa (n=10). As a control we used PLGA [poly(D,L-lactide-*co*-glycolide)]-based microspheres, as described before[20]. Two kinds of PLGA spheres were used; first, "*β-TCP-micro*" beads, containing 7.92 ± 0.20% of β-TCP [β-tricalcium phosphate] (**Fig. 8a**), second "*β-TCP/Silica-micro*" beads measuring 825 ± 30 µm, composed of 4.97 ± 0.24% β-TCP and 9.38 ± 0.53% silica. The resp. beads were pressed to 1.5 mm thick discs of a diameter of 9 mm. In previous studies it had been established that β-TCP functions as a suitable biodegradable ceramic material for bone regeneration[44]. Silica was reported by us as a promising implantconstituent with morphogenetic activity, both *in vitro*[32,33] and *in vivo*[20]. Finally microspheres had been prepared from *N,O*-CMC, solid Na-polyP and aqueous alginate "*N,O-CMC+polyP*" (**Fig. 8b**).

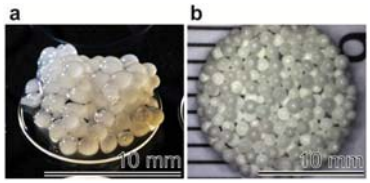

Fig. 8 Morphology of the PLGA-based microspheres. (**a**) PLGA-based microspheres, containing β-TCP, the "*β-TCP-micro*" beads. (**b**) Microspheres, prepared from *N,O*-CMC, solid Na-polyP and aqueous alginate ("*N,O-CMC+polyP*").

The implants remained in the animals for 56 d. Then the laboratory animals were sacrificed and slices were prepared from the zone of pre-existing bone-new bone and stained for mineralization using Masson's trichrome. It is evident that the samples, taken from a specimen, implanted with "*β-TCP-micro*" microspheres, are not homogenously stained in green (intensively mineralized region) but are interspersed by larger areas stained in red, indicative for the existence of non-mineralized tissue, muscle fibers and keratin (**Fig. 7d**). However, if similar samples were prepared from specimens that had received discs with microspheres containing both β-TCP and silica, "*β-TCP/Silica-micro*" beads, the green-colored areas are distinctly enlarged (**Fig. 7e**). Even more mineralization areas, almost homogeneous green staining, are seen in the areas adjacent to the pre-existing bone within the regenerated bone tissue portion (**Fig. 7f**).

In order to support and confirm the conclusion from the staining approach, the mechanical properties of the regenerating areas were determined, by using the nano-indenter technology. The experiments revealed that the pre-existing bone comprises a RedYM of 1,840 kPa, a value which is close to the bone tissue from rabbits[20]. Around the reference implant, composed of "*β-TCP-micro*" microspheres, a value of 432 kPa is measured. If β-TCP is added together with silica in the implants ("*β-TCP/Silica-micro*"), then a significant increase of the hardness to 635 kPa is measured. This morphogenetic potential has recently been also measured in the rabbit/patellar groove system[20]. Applying and implanting the new material, the "*N,O+CMC+polyP*" discs into the rat show an even significantly stronger regeneration-inducing activity with 1,475 kPa (**Fig. 7c**).

4. Conclusion

In the present work we describe the formulation and fabrication of a *N,O*-CMC-based polyP hybrid material. The two polymers are linked together *via* Ca^{2+} bridges in a stable way and provide a porous structure (**Fig. 1**). At first a homogenous suspension of *N,O*-CMC is prepared, then supplemented with solid polyP and finally mixed with aqueous alginate. This material was used for printing of the cylinders, composing the mats. Subsequently this scaffold was exposed to Ca^{2+}, resulting in a hardening of the printed biomaterial at ambient temperature. The components alginate[45], polyP (as a Na^+ salt)[46] and chitosan[47], if suspended individually in water, form random coiled structures. However, if those components are suspended in an aqueous environment and in the presence of Ca^{2+} the alginate polymers form fibers[48], *via* their clusters of α-L-guluronate residues[49]. The resulting solidified and durable cylinders cannot only be fabricated to few-layered mats, but also to more solid tissue-like units, e.g. to bioprinted implants, fitting into µCT sized lesions. Since the material retains its biological morphogenetic function, initiating biomineralization onto SaOS-2 bone-like cells, *N,O-CMC+polyP* represents a promising new material applicable in tissue engineering of bone defects by the production of personalized, custom-built bioprinted implants. The presented animal studies revealed that the newly described hybrid material *N,O*-CMC with aqueous alginate and together with the morphogenetically active polyP is, as a regeneration-inducing scaffold, also *in vivo* superior compared to β-TCP, β-TCP plus silica, described earlier.

Acknowledgements

W.E.G. M. is a holder of an ERC Advanced Investigator Grant (No. 268476 BIOSILICA). This work was supported by grants from the Deutsche Forschungsgemeinschaft (Schr 277/10-3), the European Commission ("Bio-Scaffolds: Customized Rapid Prototyping of Bioactive Scaffolds" and "BlueGenics": No. 311848) and the International Human Frontier Science Program.

Notes and references

[a] *ERC Advanced Investigator Grant Research Group at the Institute for Physiological Chemistry, University Medical Center of the Johannes Gutenberg University, Duesbergweg 6, D-55128 Mainz, GERMANY. Tel.: +49 6131-39-25910; Fax: +49 6131-39-25243; E-Mail addresses: wmueller@uni-mainz.de (Prof. W.E.G. Müller); wang013@uni-mainz.de (Prof. X.H. Wang)*
[b] *Biomaterials Department, Inorganic Chemical Industries Division, National Research Center, Doki 11884, Cairo, EGYPT*
[c] *Department of Oral and Maxillofacial Surgery, Plastic Surgery, University Medical Center of the Johannes Gutenberg University, Augustusplatz 2, D-55131 Mainz, GERMANY*

1 M. Epple and E. Bäuerlein, *Handbook of Biomineralization - Medical and Clinical Aspects*, Wiley-VCH, Weinheim, 2009.
2 K. Rezwan, Q. Z. Chen, J. J. Blaker and A. R. Boccaccini, *Biomaterials* 2006, **27**, 3413.
3 P. X. Ma, *Adv. Drug Deliv. Rev.* 2008, **60**, 184.
4 F. Croisier and C. Jérôme, *Polymer J.* 2013, **49**, 780.
5 Y. Shirosaki, K. Tsuru, S. Hayakawa, A. Osaka, M. A. Lopes, J. D. Santos, M. A. Costa and M. H. Fernandes, *Acta Biomater.* 2009, **5**, 346.
6 S. A. Smith, N. J. Mutch, D. Baskar, P. Rohloff, R. Docampo and J. H. Morrissey, *Proc. Natl. Acad. Sci. USA* 2006, **103**, 903.

7 G. Leyhausen, B. Lorenz, H. Zhu, W. Geurtsen, R. Bohnensack, W. E. G. Müller and H. C. Schröder, *J. Bone Mineral Res.* 1998, **13**, 803.

8 W. E. G. Müller, X. H. Wang, B. Diehl-Seifert, K. Kropf, U. Schloßmacher, I. Lieberwirth, G. Glasser, M. Wiens and H. C. Schröder, *Acta Biomaterialia* 2011, **7**, 2661.

9 X. H. Wang, H. C. Schröder, M. Wiens, H. Ushijima and W. E. G. Müller, *Current Opinion Biotechnol.* 2012, **23**, 570.

10 S. C. Chen, Y. C. Wu, F. L. Mi, Y. H. Lin, L. C. Yu and H. W. Sung, *J. Control Release* 2004, **96**, 285.

11 A. Anitha, V. V. Divya Rani, R. Krishna, V. Sreeja, N. Selvamurugan, S. V. Nair, H. Tamura and R. Jayakumar, *Carbohydrate Polymers* 2009, **78**, 672.

12 V. K. Mourya, N. N. Inamdar and A. Tiwari, *Adv. Mat. Lett.* 2010, **1**, 11.

13 M. Neufurth, X. H. Wang, H. C. Schröder, Q. L. Feng, B. Diehl-Seifert, T. Ziebart, R. Steffen, S. F. Wang and W. E. G. Müller, *Biomaterials* 2014, **35**, 8810.

14 K. Y. Lee and W. H. Park, *J. Appl. Polym. Sci.* 1996, **63**, 425.

15 X. P. Li, Q. Shen, Y. L. Su, F. Tian, Y. Zhao and D. J. Wang, *Cryst. Growth Des.* 2009, **9**, 3470.

16 S. A. Zijderveld, I. R. Zerbo, J. P. van den Bergh, E. A. Schulten and C. M. ten Bruggenkate, *Int. J. Oral Maxillofac. Implants* 2005, **20**, 432.

17 U. Schloßmacher, H. C. Schröder, X. H. Wang, Q. Feng, B. Diehl-Seifert, S. Neumann, A. Trautwein and W. E. G. Müller, *RSC Advances* 2013, **3**, 11185.

18 M. Mateescu, E. Rguitti, A. Ponche, M. Descamps and K. Anselme, *Biomatter.* 2012, **2**, 103.

19 C. Knabe, A. Houshmand, G. Berger, P. Ducheyne, R. Gildenhaar, I. Kranz and M. Stiller, *J. Biomed. Mater. Res.* A 2008, **84**, 856.

20 S. F. Wang, X. H. Wang, F. G. Draenert, O. Albert, H. C. Schröder, V. Mailänder, G. Mitov and W. E. G. Müller, *Bone* 2014, **67**, 292.

21 Cao L, Wang J, Hou J, Xing W, Liu C. Vascularization and bone regeneration in a critical sized defect using 2-N,6-O-sulfated chitosan nanoparticles incorporating BMP-2. *Biomaterials*. 2014, 35:684-98.

22 X. G. Chen and H. J. Park, *Carbohydrate Polymers* 2003, **53**, 355.

23 N. Sakairi, S. Suzuki, K. Ueno, S. M. Han, N. Nishi and S. Tokura, *Carbohydrate Polymers* 1998, **37**, 409.

24 X. Cui, T. Boland, D. D. D'Lima and M. K. Lotz, *Recent Pat. Drug Deliv. Formul.* 2012, **6**, 149.

25 Y. Luo, Z. Teng, X. Wang and Q. Wang, *Food Hydrocolloids* 2013, **31**, 332.

26 Y. Luo, C. Wu, A. Lode and M. Gelinsky, *Biofabrication* 2013, **5**, 015005; doi: 10.1088/1758-5082/5/1/015005.

27 T. Salge and R. Terborg, *Anadolu Univ. J. Sci. Technol.* 2009, **10**, 45.

28 D. Chavan, D. Andres and D. Iannuzzi, *Rev. Sci. Instrum.* 2011, **82**, 046107; doi: 10.1063/1.3579496.

29 D. Chavan, T. C. van de Watering, G. Gruca, J. H. Rector, K. Heeck, M. Slaman and D. Iannuzzi, *Rev. Sci. Instrum.* 2012, **83**, 115110; doi: 10.1063/1.4766959.

30 A. C. Fischer-Cripps, in *Nanoindentation, Mechanical Engineering Series 1*, Springer Science+Business Media, Berlin, 2011, pp. 21-37; DOI 10.1007/978-1-4419-9872-9_2.

31 J. Fogh, J. M. Fogh and T. Orfeo, *J. Natl. Cancer Inst.* 1977, **59**, 221.

32 M. Wiens, X. H. Wang, H. C. Schröder, U. Kolb, U. Schloßmacher, H. Ushijima and W. E. G. Müller, *Biomaterials* 2010, **31**, 7716.

33 M. Wiens, X. H. Wang, U. Schloßmacher, I. Lieberwirth, G. Glasser, H. Ushijima, H. C. Schröder and W. E. G. Müller, *Calcif. Tissue Intern.* 2010, **87**, 513.

34 WEG, Wang XH, Grebenjuk V, Diehl-Seifert B, Steffen R, Schloßmacher U, Trautwein A, Neumann S and Schröder HC (2013) Silica as a morphogenetically active inorganic polymer: effect on the BMP-2-dependent and RUNX2-independent pathway in osteoblast-like SaOS-2 cells. Biomaterials Sci. **1**: 669-678

35 Wang XH, Schröder HC, Müller WEG (2014) Properties and applications of enzymatically synthesized bio-silica. In: Springer Handbook of Marine Biotechnology; Editor - Prof. Se-Kwon Kim. Heidelberg: Springer; in press.

36 P. P. Spicer, J. D. Kretlow, S. Young, J. A. Jansen, F. K. Kasper and A. G. Mikos, *Nat. Protoc.* 2012, **7**, 1918.

37 C. Rentsch, W. Schneiders, S. Manthey, B. Rentsch and S. Rammelt, *Biomatter* 2014, **4**, e27993, doi: 10.4161/biom.27993.

38 C. C. Guedes e Silva, B. König, M. J, Carbonari, M, Yoshimoto, S. Allegrini and J. C. Bressiani, *Mater. Charact.* 2008, **59**, 1339.

39 L. Sachs, *Angewandte Statistik*, Springer, Berlin, 1984, p. 242.

40 N. H. Nie, D. H. Bent and C. H. Hull, Statistical package for the social sciences version 11.0, SPSS, Chicago, IL, USA, 2002, http://www-01.ibm.com/software/analytics/spss/.

41 J. W. Tukey, *Exploratory data analysis*, Addison-Wesley Publishing Company, 1977.

42 Hua-Cai Ge and Deng-Ke Luo, Preparation of carboxymethyl chitosan in aqueous solution under microwave irradiation. *Carbohydrate Research* 340 (2005) 1351–1356. 43 T. Kokubo, *Biomaterials* 1991, **12**, 155.

44 S. Somrani, C. Rey and M. Jemal, *J. Mater. Chem.* 2003, **13**, 888.

45 T. Andersen, J. E. Melvik, O. Gåserød, E. Alsberg and B. E. Christensen, *Carbohydr. Polym.* 2014, **99**, 249.

46 B. J. Holland, J. L. Adcock, P. N. Nesterenko, A. Peristyy, P. G. Stevenson, N. W. Barnett, X. A. Conlan and P. S. Francis, *Analyt. Chim. Acta* 2014, http://dx.doi.org/doi:10.1016/j.aca.2014.07.012.

47 G. A. Morris, J. Castile, A. Smith, G. G. Adams and S. E. Harding, *Carbohydrate Polym.* 2009, **76**, 616.

48 T. Takei, S. Sakai, H. Ijima and K. Kawakami, *Biotechnol. J.* 2006, **9**, 1014.

49 Y. Fang, S. Al-Assaf, G. O. Phillips, K. Nishinari, T. Funami, P. A. Williams and L. Li, *J. Phys. Chem. B* 2007, **111**, 2456.

In the absence of Ca^{2+} the polymers *N,O*-carboxymethyl chitosan and Na-polyphosphate, together with alginate, are present as random-coiled structures; after addition of Ca^{2+} these polymers stretch, form fibers and finally organize to durable implants.